Cu_2O-based catalysts for the electrochemical reduction of CO_2 at gas-diffusion electrodes

Jonathan Albo[a,*], *Angel Irabien*[b]

[a]*Department of Chemical Engineering, University of the Basque Country, Apdo. 644, 48080, Bilbao, Spain*

[b]*Department of Chemical & Biomolecular Engineering, University of Cantabria, Avda. Los Castros s/n, 39005, Santander, Spain*

[*]Corresponding author; e-mail: jonathan.albo@ehu.es

Abstract

Gas-diffusion electrodes are prepared with commercial Cu_2O and Cu_2O-ZnO mixtures deposited onto carbon papers and evaluated for the continuous CO_2 gas phase electroreduction in a filter-press electrochemical cell. The process mainly produced methanol, as well as ethanol and n-propanol. The analysis includes the evaluation of key variables with effect in the electroreduction process: current density (j= 10 to 40 mA·cm^{-2}), electrolyte flow/area ratio (Q_e/A= 1 to 3 ml·min^{-1}·cm^{-2}) and CO_2 gas flow/area ratio (Q_g/A= 10 to 40 ml·min^{-1}·cm^{-2}), using a 0.5 M $KHCO_3$ aqueous solution.

The maximum CO_2 conversion efficiency to liquid-phase products was 54.8% and 31.4% for Cu_2O and Cu_2O/ZnO-based electrodes, at an applied potential of -1.39 and -1.16 V vs. Ag/AgCl, respectively. Besides, the Cu_2O/ZnO electrodes are expected to catalyse the CO_2 electroreduction for over 20 h. These results may provide new insights into the development of powerful electrocatalysts for reduction of CO_2 in gas phase to alcohols.

Keywords: Electrochemical reduction, carbon dioxide, gas-diffusion electrode, copper oxide, methanol

1. Introduction

Carbon dioxide (CO_2) concentration in the atmosphere is increasing each year by about 2 mg·l^{-1}, continuing the inexorable rise toward 400 mg·l^{-1} and beyond [1]. These high atmospheric CO_2 concentrations have been now widely accepted to produce severe environmental problems such as climate change. In the 21st century our world is still

searching for strategies to overcome the challenges associated with the climate change, as well as the dependency on fossil fuels and limited natural resources.

A variety of technologies to reduce CO_2 emissions have been applied through different methods. Currently, carbon capture and storage (CCS) has received considerable attention as one of the technologies to handle large quantities of CO_2 emissions [2], where CO_2 capture seems to be the bottleneck step where the efforts have to be applied [3-5]. Sequestration has been the major storage option for CO_2 gas from power plants, but several shortcomings remain, including environmental and safety concerns about the risk of leakage and technological limitations. Thus, new approaches to mitigate carbon output from the use of fossil fuels, as well as methods to fully exploit carbon neutral renewable energy sources are needed. A possible approach to slow down the increase in atmospheric CO_2 levels is the application of electrochemical methods in a Carbon Capture and Utilization (CCU) approach [6]. This technology is green and efficient and has aroused intense attention recently. The electrochemical reduction of CO_2 can not only offer a viable route to reuse CO_2, but also a way to produce a number of valuable products, such as carbon monoxide (CO), formic acid (HCOOH), formaldehyde (CH_2O), methanol (CH_3OH), methane (CH_4), ethanol (C_2H_6O), ethylene (C_2H_4) or n-propanol (C_3H_8O) [7-9]. Particularly, the challenges for converting CO_2 into CH_3OH are great, but the potential rewards are also enormous [7, 10].

Currently, most electrodes used in the electroreduction of CO_2 are in the form of metal plates, metal granules or electrodeposited metals on a substrate [8]. However, owing to the relatively low solubility of CO_2 in water under ambient conditions, the reaction rates and current densities of CO_2 electroreduction are limited by the mass transfer of CO_2 from the bulk to the solid electrode surface [11, 12]. To improve the reduction process, gas diffusion electrodes (GDEs) have been proposed to alleviate mass transport limitations across the gas-liquid interface and to the catalyst surface [13-16]. A GDE is a porous composite electrode usually composed of polymer bonded catalyst particles and a carbon support. GDEs can be operated at higher current densities (200-600 $mA \cdot cm^{-2}$). Besides, because of their high porosity and partial hydrophobicity, GDEs form a characteristic gas-solid-liquid three-phase interface, which allows a homogeneous distribution over the catalyst surface. These properties make GDEs especially suitable for CO_2 electroreduction in gas phase.

While significant research efforts have focused on the development of new catalyst materials, considerably fewer efforts have focused on the study of these catalysts after immobilization in GDEs. In the same manner, the literature on the application of GDEs for the electrochemical transformation of CO_2 to CH_3OH is scarce [17-20]. Schwartz et al. [17] firstly studied perovskite-type crystal structures ($A_{1.8}A'_{0.2}CuO_4$, A = La, Pr and Gd; A′ = Sr and Th) in GDE for the electrochemical reduction of CO_2 under ambient conditions. The results showed that perovskite-type electrocatalysts could achieve cumulative Faradaic efficiencies for CO_2 reduction to CH_3OH, C_2H_6O, and C_3H_8O up to 40% at current densities of 180 $mA \cdot cm^{-2}$. In 2012, Aeshala et al. [18] developed Cu_2O-based GDEs by electroplating the metal particles onto a carbon paper. These materials were settled in a reactor with different solid polymer electrolytes (i.e. SPEEK, Nafion, PVA, Amberlist) for continuous gas phase CO_2 electroreduction. The maximum Faradaic efficiencies were 0.54, 0.42, 0.3, and 4.5 for CH_3OH, HCHO, CO and CH_4 production, respectively. The same group reported in 2013 a Faradaic efficiency as high as 45%, at a current density of 5.4 $mA \cdot cm^{-2}$, when applying an anionic solid polymer electrolyte membrane, with CH_3OH as the main liquid product, and CH_4 and C_2H_4 as major gaseous products. They concluded that the quaternary ammonium group in the solid polymer membrane, as well as the alleviated mass transfer limitation of CO_2 might have increase the efficiency of the GDE system [19]. Recently Lan et al. [20] investigated the electrochemical reduction of CO_2 on a Cu(core)/CuO(shell) catalyst in a flow reactor. This catalyst predominantly produce CO and HCOOH at 54.6 $mA \cdot cm^{-2}$, with a Faradaic efficiency of 21.5% and 20.2%, respectively. However, a small amount of CH_3OH was also produced in the process (~2.5% Faradaic efficiency).

Furthermore, the literature demonstrated the good stability and notable catalytic ability of Cu_2O-based surfaces for electrochemical hydrocarbons and/or alcohols formation from CO_2 [8, 11, 17-25]. Besides, the inclusion of ZnO may be the key for maintaining catalytic activity, since ZnO strengthen the Cu-CO^- link, increasing the selectivity to alcohols, and stabilizing Cu in the hydrogenation reaction [11, 26-29]. Therefore, the primary objective of this study is to evaluate the performance of GDEs with spray supported Cu_2O and Cu_2O/ZnO catalysts for the continuous electroreduction of CO_2 in gas phase. Then, an evaluation of the influence of key variables on the CO_2 electroreducion process (i.e. current density, electrolyte flow and CO_2 gas flow) is performed. The results are compared to those obtained in our previous work, where

mass transfer limitations were detected in the electroreduction of CO_2 in liquid phase when using a filter-press electrochemical cell.

The efforts carried out in this work will help to achieve the scale-up of CO_2 valorisation processes and devices in continuous operation, enabling a shift to a sustainable energy economy and chemical industry.

2. Materials and methods

2.1. Preparation and characterization of the gas-diffusion electrodes

The procedure to prepare the Cu_2O and Cu_2O/ZnO GDEs has been described in detail previously [11]. The Cu_2O-GDEs contain 1 $mg{\cdot}cm^{-2}$ of metal particles. The catalyst loading was kept at 1 $mg{\cdot}cm^{-2}$ of Cu_2O and 1 $mg{\cdot}cm^{-2}$ of ZnO for the Cu_2O/ZnO electrodes. Briefly the procedure is as follows; Cu_2O (Sigma Aldrich, particle size < 5 µm, 97% purity) and ZnO particles (ACROS organic, < 45 µm, 99.5%) were mixed with a Nafion® dispersion 5 wt.% (Alfa Aesar) and isopropanol (IPA) (Sigma Aldrich), with a 70/30 catalyst/Nafion mass ratio and a 3% solids (catalyst + Nafion). This ink was airbrushed onto a porous carbon paper (TGP-H-60, Toray Inc.) and dried to get the electrodes. All electrodes were dried and rinsed with deionised water before use.

The EDX spectra and surface mapping confirmed the composition and uniform distribution of Cu_2O-ZnO metal particles onto the carbon paper (See Figure A in Supporting Information). Thus, it can be inferred that the dispersion of the particles by air-brushing minimizes the agglomeration of the particles, which may greatly affect the electrode performance [23, 24, 29]. Besides the SEM cross-section image of the GDE shows that the diffusion layer (carbon paper) and the catalytic layer (Cu_2O-ZnO) combined with each other tightly and the metallic particles covered nearly the entire carbon fibers of the support (See Figure B in Supporting Information).

2.2. Electrochemical cell and experimental conditions

The components of the experimental setup have been described in detail elsewhere [13]. The electroreduction of CO_2 was carried out at ambient conditions using a filter-press electrochemical cell (Micro Flow Cell, ElectroCell A/S) in continuous operation. The cell was divided in a catholyte and anolyte compartments by a Nafion 117 cation exchange membrane. The membrane was treated prior the use following standard

procedures [30]. The airbrushed Cu_2O and Cu_2O/ZnO-catalysed papers were employed as the working electrodes (geometric area, A= 10 cm^{-2}), together with a platinised titanium plate used as the counter electrode and a Ag/AgCl (sat. KCl) reference electrode.

The cathode side of the reactor was fed with CO_2 gas (99.99%) with a flow/area ratio ranging from 10 to 40 $ml \cdot min^{-1} \cdot cm^{-2}$, adjusted by a rotameter. A 0.5 M $KHCO_3$ (Panreac) aqueous solution is used as both, catholyte and anolyte, with a flow rate ranging from 1 to 3 $ml \cdot min^{-1} \cdot cm^{-2}$. The electrolytes were pumped from catholyte and anolyte tanks to the cell by two peristaltic pumps (Watson Marlow 320, Watson Marlow Pumps Group). In this study, the filter-press electrochemical system possesses three inputs (catholyte, anolyte and CO_2 separately) and two outputs (catholyte-CO_2 and anolyte) for the electroreduction of CO_2 in gas phase. Figure 1 schematically represents the electrolytic GDE cell configuration for the electroreduction of CO_2 supplied directly from the gas phase.

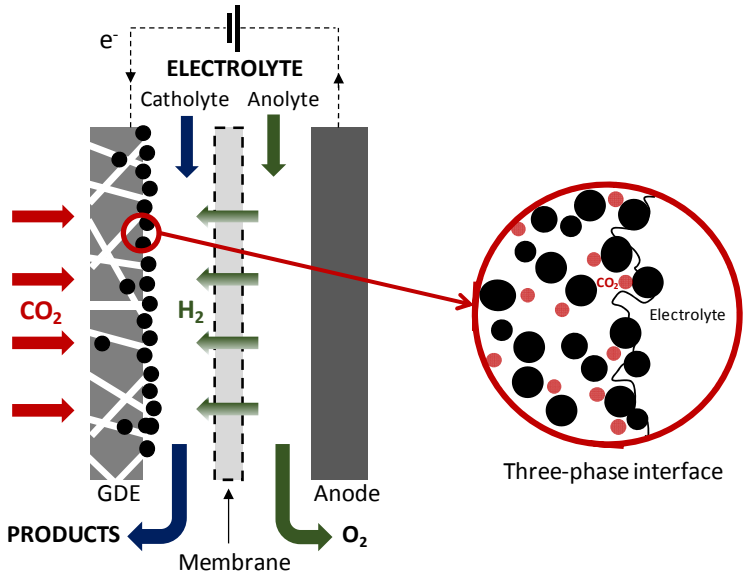

Fig. 1. Schematic diagram of the electrolytic cell configuration for the electroreduction of CO_2 supplied directly from the gas phase

The experiments were performed at galvanostatic conditions (i.e. at a constant current density), using an AutoLab PGSTAT 302N potentiostat (Metrohm, Autolab B.V.). The current density ranged from j= 5 to 40 $mA \cdot cm^{-2}$ in the electrochemical experiments. Liquid samples were taken every 15 minutes from the catholyte tank with a total

operational time of 90 minutes, where pseudo-stable values are obtained [11]. All the experiments were carried out at ambient conditions.

To quantify the concentration of each product in the liquid phase, the samples were analysed by duplicate in a headspace gas chromatograph (GCMS-QP2010, Ultra Shimadzu) equipped with a flame ionization detector (FID). Compounds were separated on a DB-Wax 30 m x 0.25 mm x 0.25 µm column, with an injection and detector temperature of 250 ºC and 270 ºC, respectively. Helium was used as a carrier gas at a flow rate of 50 $ml \cdot min^{-1}$. The identification of obtained products was further confirmed by headspace gas chromatography-mass spectrometry (GCMS-N5975B) using a 60 m x 250 µm x 1.40 µm DB-624 capillary column. Three replicates were performed for each sample to obtain an averaged concentration of the formed products. The standard deviations of all the experiments were below 18.6 %.

The performance of the electrochemical process is evaluated by the rate of product formation, *r* (i.e. product obtained per unit of cathode area and time), and the Faradaic efficiency, *FE* (i.e. selectivity of the reaction for the production of each product). The *FE* represents the percentage of the total charge supplied to the system that is used to form the different products.

3. Results and discussion

3.1. Continuous electroreduction of CO_2 in a filter-press electrochemical cell

The electroreduction of CO_2 at the Cu_2O-based GDEs led predominantly to the formation of CH_3OH, in accordance to those previous results at copper oxides surfaces [11, 24, 25]. Additionally, small quantities of C_2H_6O and C_3H_8O were also detected. Figure 2 shows the course of the applied voltage, *E*, and formation rate, *r*, of the main liquid-phase product, CH_3OH, over time for the CO_2 electroreduction at both electrodes at ambient conditions.

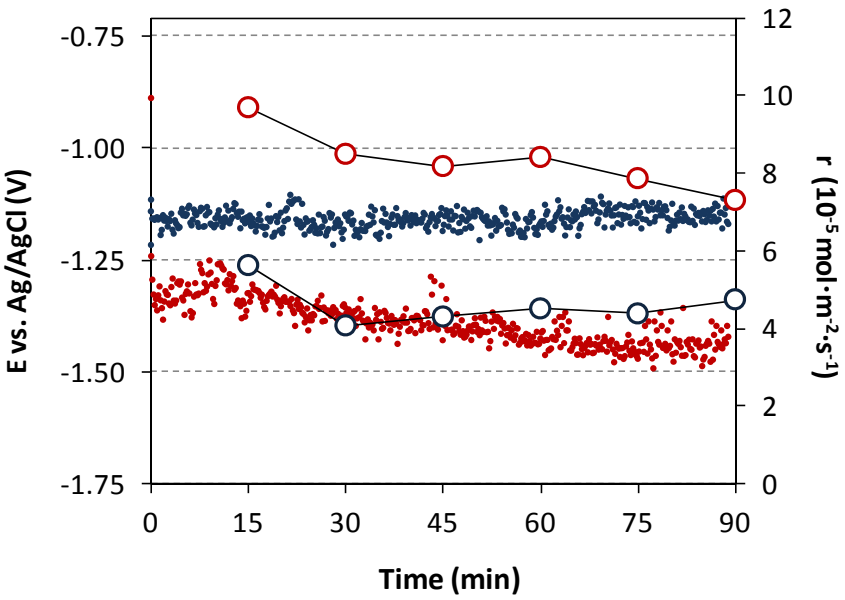

Fig. 2. Electrocatalytic activity for the conversion of CO_2 at Cu_2O (in red) and Cu_2O/ZnO (in blue) GDEs. The figure shows the applied voltage, *E*, for a constant current of *j*= 10mA·cm^{-2} and the averaged rate of CH_3OH formation, *r*, with time.

From the figure, the required voltage, *E*, remains stable for the Cu_2O/ZnO-based electrodes over the course of the 90 minutes of operation. In contrast, the Cu_2O electrode required an increasing applied voltage to maintain a stable current (*j*= 10 mA·cm^{-2}), which may be related to the progressive detachment of catalyst particles from the GDE surface and the deactivation due to the exposure to concentrated CO_2 gas [31, 32]. The observed fluctuations in required voltage can be explained as bubbles are formed on the electrode surface, especially at Cu_2O-based GDEs, where higher potentials are required (*E*= -1.25 to -1.50 V vs. Ag/AgCl), in comparison to the application of Cu_2O/ZnO mixtures airbrushed onto the carbon papers (*E*= -1.16 V vs. Ag/AgCl). The lower potentials needed for Cu_2O-ZnO mixtures are in agreement with the higher cyclic voltammetry responses reported for Cu_2O/ZnO-based electrodes in comparison to those electrodes with deposited Cu_2O particles, denoting the synergic effect of Cu_2O and ZnO in the current-potential reduction response [11].

Moreover, the rate of CH_3OH formation, *r*, decreased for both electrodes as time went on, and then stabilize uniquely for Cu_2O/ZnO layers after 30 minutes of reaction at *r*= ~4 x 10^{-5} mol·m^{-2}·s^{-1} until the end of the experiment. Probably, at the first experimental minutes, the electrolyte penetrated into the internal structure of the GDE, enlarging the contact area. This may explain the enhanced reaction rate at 15 min of operation,

indicating that the structure is sufficiently soaked and the three-phase liquid films had totally formed thoroughly the whole GDEs [33]. After this point, the GDE probably was to wet, limiting mass transfer to some extent and accumulating liquid-phase reaction products, which can partially block the electrode and reduce its electrochemically-active surface area [34-36]. Therefore, a gradual infiltration of electrolyte may be preferred for an enhanced CO_2 conversion at GDEs.

Table 1 shows the catalyst weight of the Cu-based samples after 30, 90 and 120 min of CO_2 electroreduction time. The total weight of catalyst placed in the carbon paper was 10 mg and 20 mg for Cu_2O and Cu_2O/ZnO-based electrodes, respectively.

Table 1. Particle loss for Cu_2O and Cu_2O/ZnO GDEs before and after a CO_2 electroreduction period of 30, 90 and 120 min.

Electrode	**Time (min)**	**Catalyst weight (mg)**		**Weight loss (%)**
		Initial	Final	
Cu_2O	30	10	9.04	9.56
	60		8.55	14.54
	90		7.97	20.35
Cu_2O/ZnO	30	20	19.04	4.82
	60		18.72	6.41
	90		18.61	6.97

The results confirmed the more stable propierties of Cu_2O/ZnO surfaces in comparison to the Cu_2O-based electrode, where the catalysts may be gradually peeled off from the carbon paper. Besides, defects in the catalytic layer would likely assist tunnelling and an increase the unwanted hydrogen formation due to easy access of water to catalytic sites. Therefore, a uniform and defect free catalyst layer is desired [16, 21]. According to the results, it is expected that Cu_2O/ZnO layer could remain and catalyse the CO_2 electroreduction for over 20 h (if we consider the same particle detachment rate), since the total particle loss at 90 min was 1.39 mg of a total of 20 mg sprayed in the electrode. Overall, even if the Cu_2O-based GDEs present an initial better performance for CH_3OH formation, the utilization of Cu_2O-ZnO mixtures is recommended for a continuous CO_2 electrochemical conversion due to its stable properties with time.

The averaged formation rate for Cu_2O/ZnO surfaces at 90 min of operation takes the value of r= 4.74 x 10^{-5} mol·m^{-2}·s^{-1}, which is higher than that value reported in our previous work at Cu_2O/ZnO particles deposited onto carbon papers (without the supply of CO_2 gas), r= 3.17 x 10^{-5} mol·m^{-2}·s^{-1} [11]. Besides, the stable formation rate obtained at Cu_2O/ZnO-based electrode is in the range of those values previously reported for air-furnace oxidized Cu foils (r= 2.36 x 10^{-5} mol·m^{-2}·s^{-1}) and electrochemical oxidized Cu foils (r= 2.78 x 10^{-5} mol·m^{-2}·s^{-1}) at potentials ranging from -1.2 to -1.5 V vs. Ag/AgCl [21] or the CH_3OH formation rates reached at electrodes based on Cu_2O electrodeposited on stainless steel, r= 11.9 x 10^{-5} mol·m^{-2}·s^{-1} at -1.05 V vs. Ag/AgCl [25].

3.2. Key variables on the CO_2 electroreduction process

This section analyzes the influence of current density, j; electrolyte flow/area ratio (Q_e/A) and gas flow/area ratio (Q_g/A) in the liquid-phase product distribution and the CO_2 conversion efficiency for the filter-press electrochemical system in continuous operation.

3.2.1. Influence of current density

Figure 3 shows the quantitative information (r and FE) regarding the liquid-phase product distribution at different current densities (j= 5 to 40 mA·cm^{-2}). FE was calculated considering 6 electrons step pathways of CO_2 reduction to CH_3OH, 12 electrons required per molecule of ethanol (C_2H_6O) and 18 to produce n-propanol (C_3H_8O). A constant electrolyte flow/area ratio (Q_e/A) and gas flow/area ratio (Q_g/A) of 2 and 20 ml·min^{-1}·cm^{-2}, respectively, were applied in the tests. It may be noted that the carbon paper without metallic particles supported did not produce any measurable liquid product.

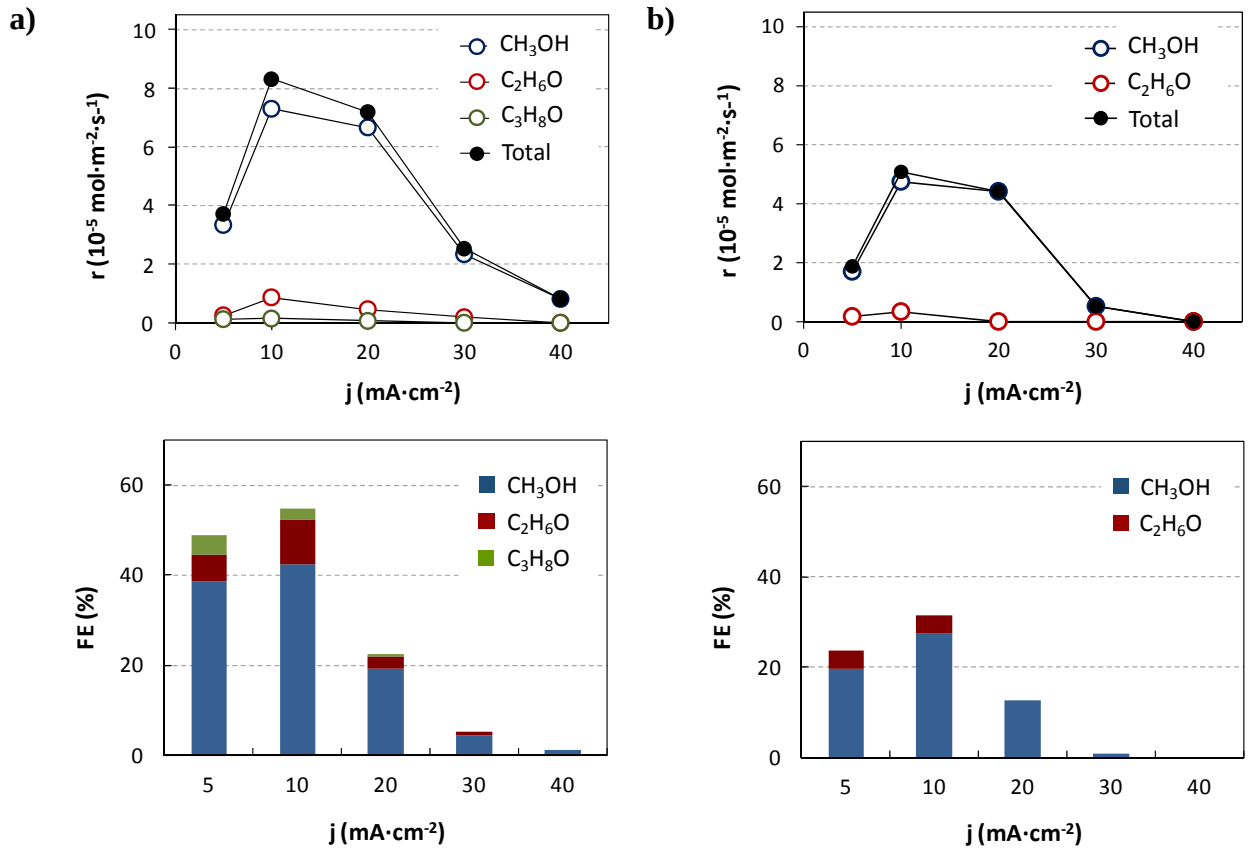

Fig. 3. Rates of product formation, *r*, and Faraday efficiencies, *FE*, for the major products obtained from CO_2 electroreduction at (a) Cu_2O and; (b) Cu_2O/ZnO-GDEs as a function of current density applied.

The figures show that the product distribution and process efficiency is on dependence of the current density applied. The system predominantly produces CH_3OH, with C_2H_6O as the second main product (which is a difficult reaction with 12 electrons transfer required). The literature shows that the formation of C_2H_6O at Cu-based electrodes is not unexpected [9, 37-42]. For example, Chi et al. [38] reported a good selectivity for the formation of C_2H_6O (*FE*= 15.5%) for CuO nanoparticles deposited on carbon papers when using a 0.2 M $KHCO_3$ solution. Trace amounts of CH_3OH and C_3H_8O were also detected. Ren et al. [40] recently reported the formation of C_2 compounds (C_2H_6O and C_2H_4) on Cu_2O films at various electrochemical potentials. The *FE* was in the range of 9-16% for C_2H_6O formation in a 0.1 M $KHCO_3$ electrolyte. They hypothesized that CO_2 is reduced through proton-electron transfer to give $HCOO^-$ surface moiety, which can then hydrogenate to give H_2O and CO (adsorbed) at the copper surface. These species can further hydrogenate to form CH_4 or undergo intermolecular C-C bound formation (C_1 dimerization/hydrogenation) to yield $C_2H_nO_2$ (n= 0-4), which is further reduce to C_2H_6O and C_2H_4. The Cu^+ ions were postulated to

be the catalytic active for reducing CO_2 to C_2 compounds. Besides, Li and co-workers demonstrated that Cu_2O films could reduce CO to C_2H_6O with a *FE* of 43% [41]. The metal particles boundaries on the surface (with undercoordinated Cu atoms) of the films were suggested to be the driving forces for C_1 dimerization to form C_2 products. Moreover, Kuhl et al. [9] evaluated the electrochemical reduction of CO_2 on a Cu surface across a range of potentials and observed a total of 16 different CO_2 reduction products (including CH_3OH, C_2H_6O and C_3H_8O). They discuss a scheme for the formation of multicarbon products and recognized that all the C_2 and C_3 products detected may have been produced via the dehydroxylation of an earlier, less reduced product in its enol or diol form. Therefore, they hypothesized that the chemistry to generate the wide range of multicarbon products may occur through an enol-like surface intermediate, that desorb to convert to its diol and/or keton form. The presence of hydroxyl and/or carbonyl moieties in many of the C_2 and C_3 products suggest that the C-C coupling step occurs before at least one of the two carbon-oxygen bonds in CO_2 is broken. In any case, the mechanisms involved in C-C coupling reactions to form C_2 and C_3 products are still unclear. Certainly, further experimental work is needed to fully elucidate CO_2 reduction steps on Cu surfaces.

The results also suggest that the reaction conditions created in the GDEs may be able to vary product selectivity if we compare the results with those obtained at identical catalytic materials but without CO_2 supplied as gas, where CH_3OH was the main product, and only trace amounts of C_2H_6O were detected [11]. This is not exceptional if we consider those results obtained by Kas et al. for electrodes prepared with Cu nanoparticles for CO_2 electroreduction to hydrocarbons [39, 42]. They proved that identical electrodes could yield predominately CH_4 and C_2H_4 depending on process conditions, such as the applied CO_2 pressure, that can modify the conditions in the vicinity of the catalytic material. In theory, the GDE configuration changes CO_2 transfer radically. Owing to the abundant pores in the GDEs, CO_2 can diffuse to the electrode surface more conveniently than that from the bulk. Moreover, CO_2 in the reaction can be obtained from CO_2 (gas), rather that CO_2 (aqueous) by use of GDEs, so that the concentration of CO_2 (adsorbate) on the electrode surface can be increased [34] which probably may lead to the formation of more reduced species, altering the distribution of products from the reaction. It is also interesting to note the positive effects of supplying a CO_2 gas flow through the electrode structure, which may provoke that the liquid

products diffuse more easily to the solution, avoiding the entrapment of liquid products into the carbon paper porous structure. Further research is required to fully understand this phenomenon.

Figure 3a and b reveal that the total rate of CO_2 reduction to liquid-phase products, r_T, did not improve at current densities higher than j= 10 mA·cm^{-2}, where a maximum value of r_T= 8.32 x 10^{-5} mol·m^{-2}·s^{-1} and r_T= 5.08 x 10^{-5} mol·m^{-2}·s^{-1} can be obtained at Cu_2O and Cu_2O/ZnO-based electrodes, respectively. In addition, the overall FE_T (the results of cumulative efficiencies for the formation of the different products) fell drastically as the current was increased from j= 10 to 40 mA.cm^{-2}. This may be explained as the additional current density applied is consumed by side reactions, such as the production of hydrogen (which competes with the electroreduction of CO_2 to useful products) and may indicate an optimal electrocatalytic current density of j= 10 mA·cm^{-2}, where the overall efficiency values can be as high as FE_T = 54.8% and 31.4% for the Cu_2O and Cu_2O/ZnO-based surfaces, respectively.

Moreover, Table 2 compares the product distribution and *FE* for CO_2 conversion obtained in the present work with those previously obtained for the same materials in a CO_2-saturated 0.5 M $KHCO_3$ solution (without CO_2 supplied as gas) [11]. The performance is, at the same time, compared with the values obtained in a CO_2-saturated 0.5 M $KHCO_3$ solution when N_2 gas is supplied through the GDE structure (instead of CO_2).

Table 2. Electrochemical reduction of CO_2 at Cu_2O and Cu_2O/ZnO electrodes when CO_2 and N_2 gas flow through the GDE, and when no gas is supplied. Electrolyte flow/area ratio (Q_e/A)= 2 ml·min^{-1}·cm^{-2}. Gas flow ratio (Q_g/A)= 20 ml·min^{-1}·cm^{-2}.

Electrode	**Flowing gas**	***j* (mA·cm^{-2})**	***E* vs. Ag/AgCl**	**FE (%)**			
				CH_3OH	C_2H_6O	C_3H_8O	Total
Cu_2O	CO_2	10	1.39	42.3	10.1	2.4	54.8
	N_2	10	1.52	40.2	2.3	-	42.5
	-	6.93[a]	1.30	45.7	Trace	-	45.7
Cu_2O/ZnO	CO_2	10	1.16	27.5	3.9	-	31.4
	N_2	10	1.69	18	1.5	-	19.5
	-	10.64[a]	1.30	17.7	Trace	-	17.7

[a] Data from ref. [11]

The overall *FE* achieved for the conversion of CO_2 demonstrated that the GDE with CO_2 gas feeding to the electrocatalysts contributed to the high electrolysis efficiency, as compared to those results obtained at the identical electrodes when no CO_2 as gas is supplied [11]. Besides, as observed from the results, the Cu_2O-GDE maintained a higher efficiency for CO_2 reduction (FE_T= 54.8%) at higher current density (j=10 mA·cm^{-2}) than at Cu_2O-surfaces (FE_T= 45.7%) at lower current applied (j= 6.93 mA·cm^{-2}). This may indicate that the application of GDEs (with CO_2 supplied as gas) is advantageous, since the process can be operated at higher current densities, while yielding higher CO_2 reduction efficiencies.

Moreover, the efficiency values for the conversion of CO_2 at GDEs are remarkably higher than those values obtained at a CO_2-saturated solution when N_2 gas is supplied through the GDE structure, which suggest that the conversion of CO_2 molecule can be not uniquely attributed to an enhanced agitation and diffusion of reactants in the electrochemical cell, but also to an increase of CO_2 (adsorbate) available on the catalytic surface, leading to more reduced species.

3.2.2. Influence of electrolyte flow rate (Q_e/A) and gas flow rate (Q_g/A)

In our previous study, external mass transfer limitations were detected in the filter-press electrochemical cell system [11], which might be overcome with the application of GDEs [13-16]. In order to improve the CO_2 electroreduction performance, additional experiments were carried out at different electrolyte flow/area ratio (Q_e/A) and CO_2 gas flow/area ratio (Q_g/A) and the results for the formation of the major product, CH_3OH, are presented in Figure 4a and b, respectively.

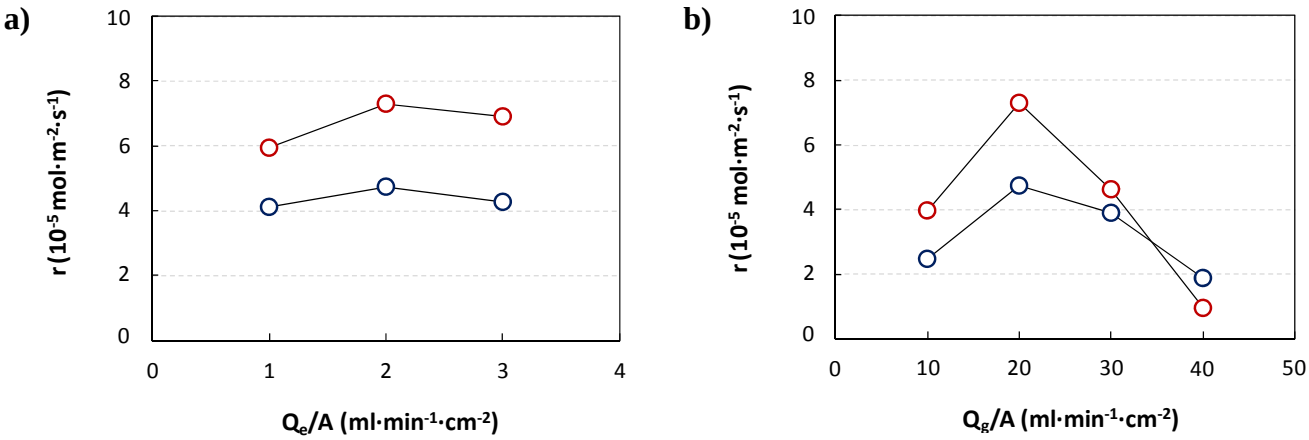

Fig. 4. Rate for CO_2 reduction to CH_3OH, *r*, at (a) different electrolyte flow rate (Q_e/A) and; (b) CO_2 gas flow rate (Q_g/A) at the Cu_2O (in red) and Cu_2O/ZnO (in blue) GDEs. Current density: j= 10 mA·cm^{-2}

Firstly, Figure 4a shows that increases in Q_e/A from 1 to 3 ml·min^{-1} did not produce a significant alteration in the rate of CO_2 electrochemical conversion to CH_3OH, which indicated that using low Q_e/A ratios is preferred in the GDE system since a more concentrated product can be obtained without sacrificing the rate of CH_3OH formation (i.e. from 4.56 to 2.74 mg·l^{-1} at Q_e/A= 2 and 3 ml·min^{-1}, respectively, at Cu_2O/ZnO GDE). Besides, lower electrolyte flows may allow a gradual infiltration of catholyte in the GDE structure, which is preferred for an enhanced CO_2 electroreduction, as discussed in section 3.1. Therefore, since process performance was only slightly affected by the electrolyte flow, it can be concluded that the process may be primarily limited by the internal diffusion of reactants through the porous structure of the GDE, where the metal particles are deposited [13].

Additionally, Figure 4b demonstrated the importance of adjusts the optimal CO_2 gas flow process. The lower formation rate (r= 2.48 x 10^{-5} mol·m^{-2}·s^{-1}) for Cu_2O/ZnO-based electrode at Q_g/A= 10 ml·min^{-1}·cm^{-2} in comparison to that value at Q_g/A= 20 ml·min^{-1}·cm^{-2} (r= 4.74 x 10^{-5} mol·m^{-2}·s^{-1}) indicated that the process is clearly limited by the CO_2 gas supplied to the system. On the other hand, the application of a high CO_2 gas flow of Q_g/A= 40 ml·min^{-1}·cm^{-2} produced a severe decrease in the formation rate for both electrodes, which can be partially attributed to the rapid detachment of metal particles at these relatively high gas flows applied, in accordance with the main stability limitations observed in GDE systems [15, 31, 43].

Therefore, the optimal point should provide enough CO_2 gas supply for the reaction, well before a massive detachment of metal particles occurrs. This seems to happen at a flow range between Q_g/A= 20 to 30 ml·min^{-1}·cm^{-2}. These results are interesting and should be taken into account in order to design efficient processes for CO_2 eletroreduction to CH_3OH at GDE-based systems.

3.3. Comparison with other electrocatalytic materials

Finally, the results obtained in the present work for Cu_2O and Cu_2O/ZnO-GDEs are compared with previous results for CO_2 electroreduction to liquid products at different Cu-based materials (when boht, *r* and *FE,* values available) at an applied potential range of *E*= -1 to -1.5 vs. V Ag/AgCl [11, 21, 25, 29]. Figure 5 represents the total rate of CO_2 conversion, r_T, vs. cumulative Faradaic efficiency, FE_T, reported in the literature for the formation of different liquid-phase products, including CH_3OH. The figure uniquely provide a picture for comparison of CO_2 electroreduction performance, although other variables such as reaction medium, operating conditions and/or cell/electrode structure were applied, which may affect the results. The extraordinary high FE (i.e. >100%), where obiously both chemical and electrochemical steps involved in the CO_2 reduction process, obtained at anodized Cu foils and pre-oxidized Cu-TiO_X electrodes [21] have been not included in order to clarify the analysis.

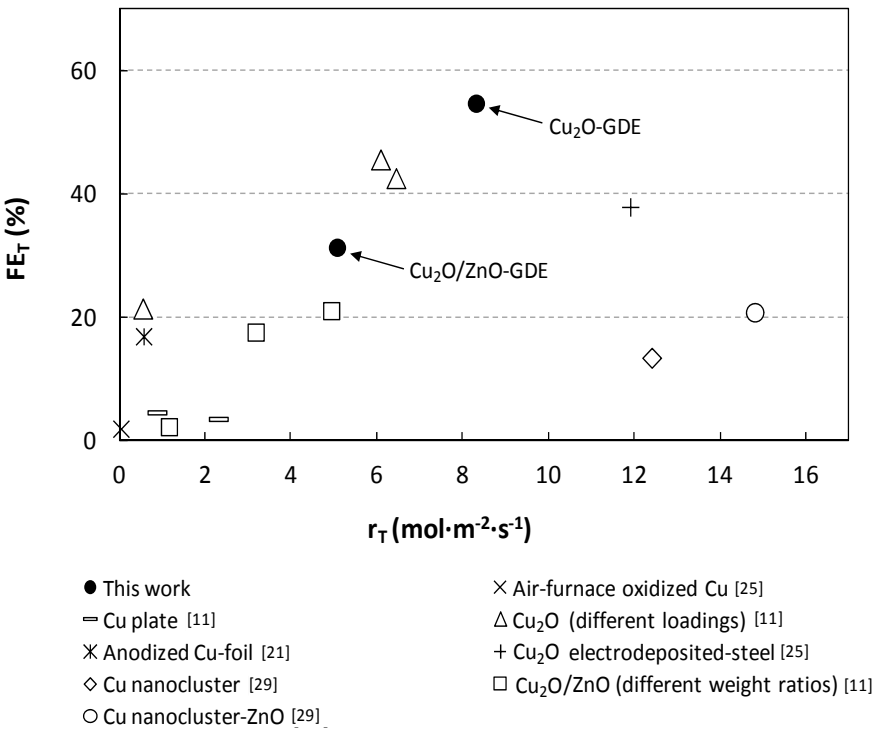

Fig. 5. Total rate of CO_2 conversion to liquid-phase products, r_T, vs. Faradaic efficiency, FE_T, for different Cu-based materials at E= -1 to -1.5 V vs. Ag/AgCl

As can be seen from the figure, the total CO_2 conversion efficiency obtained for GDEs in the present work outperformed those values observed at Cu, oxidized Cu and Cu-Zn surfaces, which may denote the positive effect of using GDEs. Nevertheless, the rate of CO_2 reduction to useful products is still below those values reported for Cu_2O electrodeposited-steel electrode, r_T= 11.9 x 10^{-5} mol·m^{-2}·s^{-1} at -1.05 V vs. Ag/AgCl [25] or those values for Cu nanoclusters-ZnO mixtures at -1.4 V, where high total formation rates, r_T= 12.4 - 14.8 x 10^{-5} mol·m^{-2}·s^{-1}, were reached. In any case, the relatively high CO_2 conversion rate to liquid products, r_T= 5.08 x 10^{-5} mol·m^{-2}·s^{-1} and total Faradaic efficiency, FE_T= 31.4%, as well as the stable behavior, suggest the use of Cu_2O/ZnO-based GDEs for the continuous electrochemical reduction of CO_2 to useful products, where CH_3OH is the predominant product.

Future research should probably include the development of new highly active catalysts, as well as a deeper study to understand the relationship between GDE morphology and effective gas-liquid separation, while facilitating transport of reactants and products. These progresses may lead in the near future to an economically-viable CO_2 electrochemical process in continuous operation.

4. Conclusions

This work demonstrated that the electroreduction of CO_2 to liquid products can be effectively carried out in continuous in a filter-press electrochemical cell equipped with Cu_2O-based gas-diffusion electrodes (GDEs). The GDE configuration allows breaking through the mass transfer limitations usually found in electroreduction systems, producing an enhanced CO_2 reduction performance. The study included the experimental evaluation of key variables (i.e. current density, j; electrolyte flow/area ratio, Q_e/A; and CO_2 gas flow rate/area ratio, Q_g/A) for the electrochemical conversion of CO_2 at Cu_2O and Cu_2O/ZnO commercial particles deposited onto carbon papers in a 0.5 M $KHCO_3$ catholyte under ambient conditions.

The experimental results in the filter-press electrochemical cell revealed that Cu_2O/ZnO-GDEs are expected to remain stable over 20 h, in contrast to Cu_2O surfaces that suffered a strong deactivation with time. The analysis of the liquid catholyte demonstrated that methanol was formed predominantly, with small amounts of ethanol and n-propanol.

The overall formation rate for the formation of liquid-phase products did not improve at current densities higher than j= 10 mA·cm^{-2}, where a maximum value of r_T= 5.08 x 10^{-5} mol·m^{-2}·s^{-1} was obtained at Cu_2O/ZnO-GDEs. In addition, the overall FE (the results of cumulative efficiencies for the formation of the different products) fell drastically as the current was increased from j= 10 to 40 mA·cm^{-2}. The process performance was not affected by electrolyte flow, suggesting that the process may be primarily limited by the internal diffusion of reactants through the porous structure of the GDE, where the metal particles are deposited. In addition, the results demonstrated the importance of adjusting the optimal CO_2 gas flow in the electrochemical cell in order to supply enough CO_2 to react before a rapid detachment of metal particles from the catalytic surface occurred. Thus, the maximum efficiency detected at Cu_2O/ZnO surfaces was FE_T= 31.4% (at j= 10 mA·cm^{-2}, Q_e/A= 2 ml·min^{-1}·cm^{-2} and Q_g/A= 20 ml·min^{-1}·cm^{-2}), which is a significantly higher value than those results previously reported in literature for Cu-based electrodes and show the potential of Cu_2O/ZnO-GDEs for the effective electrochemical valorization of CO_2.

Overall, the results presented in this work are promising, but research efforts must be continued in order to develop new electroreduction systems based on highly active,

selective and stable materials to overcome the current limitations of the process before practical applications.

Acknowledgements

The authors gratefully acknowledge the financial support from the Spanish Ministry of Economy and Competitiveness (MINECO), under the projects CTQ2013-48280-C3-1-R, CTQ2013-48280-C3-3-R and *Juan de la Cierva* program (JCI-2012-12073). The authors would like to express their appreciation to Alfonso Sáez, Jose Solla-Gullón and Vicente Montiel (Institute of Electrochemistry, University of Alicante, Spain) for their assistance in the characterization of the material.

References

[1] CO_2 Emissions From Fuel Combustion Highlights 2014, *International Energy Agency (IEA)*, **2014**.

[2] M.E. Boot-Handford, J. C. Abanades, E.J. Anthony, M.J. Blunt, S. Brandani, N. Mac Dowell, J.R. Fernandez , M.C. Ferrari, R. Gross, J.P. Hallet, R.S. Haszeldine, P. Heptonstall, A. Lyngfelt, Z. Makuch, E. Mangano, R.T.J. Porter, M. Pourkashanian, G.T. Rochelle, N. Shah, J.G. Yao, P.S. Fenell, *Energ. Environ. Sci.* 7, **2014**, 130-189.

[3] J. Albo, T. Yoshioka, T. Tsuru, *Sep. Purif. Technol*., 122, **2014**, 440-448.

[4] J. Albo, A. Irabien, *J. Chem. Technol. Biot*., 87:10, **2012**, 1502-1507.

[5] J. Albo, P. Luis, A. Irabien, *Ind. Eng. Chem. Res.*, 49:21, **2010**, 11045-11051.

[6] M. Cuéllar-Franca, A. Azapagic, *Journal of CO_2 Utilization*, 9, **2015**, 82-102.

[7] J. Albo, M. Alvarez-Guerra, P. Castaño, *Green Chem*., 17, **2015**, 2304-2324.

[8] J. Qiao, Y. Liu, F. Hong, J. Zhang, *Chem. Soc. Rev*., 43, **2014**, 631-675.

[9] K. P. Kuhl, E. R. Cave, D. N. Abram, T. J. Jaramillo, *Energ. Environ. Sci.*, 5, **2015**, 7050-7059.

[10] G.A. Olah, *Angew. Chem., Int. Ed*., 44, **2005**, 2636-2639.

[11] J. Albo, A. Sáez, J. Solla-Gullón, V. Montiel, A. Irabien, *Appl. Catal. B-Environ.*, **2015**, DOI: 10.1016/j.apcatb.2015.04.055.

[12] M. Alvarez-Guerra, S. Quintanilla, A. Irabien, *Chem. Eng. J.*, 207, **2012**, 278-284.

[13] A. Del Castillo, M. Alvarez-Guerra, A. Irabien, *AIChE J.*, 60:10, **2014**, 3557-3564.

[14] Q. Wang, H. Dong, H. Yu, *RSC Adv.*, 4, **2014**, 59970-59976.

[15] Q. Wang, H. Dong, H. Yu, *J. Power Sources*, 271, **2014**, 278-284.

[16] H-R. Jhong, F. R. Brushett, P. A. Kenis, *Adv. Energy Mater.*, 3, **2013**, 589-599.

[17] M. Schwartz, R. L. Cook, V. M. Kehoe, R. C. Macduff, J. Patel, A. F. Sammells, *J. Electrochem. Soc.,* 140, **1993**, 614-618.

[18] L. M. Aeshala, S.U. Rahman, A. Verma, *Sep. Purif. Technol*. 94, **2012**, 131-137.

[19] L. M. Aeshala, R.G. Uppaluri, A. Verma, *Journal of CO_2 Utilization*. 3-4, **2013**, 49-55.

[20] Y. Lan, S. Ma, J. Lu, P. J. A. Kenis, , *Int. J. Electrochem. Sci*., 9, **2014**, 7300-7308.

[21] K. W. Frese, *J. Electrochem. Soc.* 138:11, **1991**, 3338-3344.

[22] M. Gattrell, N. Gupta, A. Co, *J. Electroanal. Chem.*, 594, **2006**, 1-19.

[23] S. Ohya, S. Kaneco, H. Katsumata, T. Suzuki, K. Ohta, *Catal. Today.,* 148, **2009**, 329-334.

[24] T. Y. Chang, R. M. Liang, P. W. Wu, J. Y. Chen, Y. C. Hsieh, *Mat. Lett*. 63, **2009**, 1001-1003.

[25] M. Le, M. Ren, Z. Zhang, P. T. Sprunger, R. L. Kurtz, J. C. Flake, *J. Electrochem. Soc*., 158:5, **2011**, E45-E49.

[26] M. S. Spencer, *Top. Catal.,* 8, **1999**, 259-266.

[27] H. Nakatsuji, Z.M. Hu, *Int. J. Quantum Chem.,* 77, **2000**, 341-349.

[28] Y. Yang, J. Evans, J. Rodriguez, M.G. White, P. Liu, *Phys. Chem. Chem. Phys.* 12 , **2010**, 9909-9917.

[29] E. Andrews, M. Ren, F. Wang, Z. Zhang, P. Sprunger, R. Kurtz, J. Flake, *J. Electrochem. Soc*., 160:11, **2013**, H841-H846.

[30] G. Q. Lu, C. Y. Wang, T. J. Yen, X. Zhang, *Electrochimica Acta*, 49, **2004**, 821-828.

[31] S. Lee, H. Ju, R. Machunda, S. Uhm, J. Kwang Lee, H. Jin Lee, J. Lee, *J. Mater. Chem. A.,* 3, **2015**, 3029-3034.

[32] R. L. Machunda, H. Ju, J. Lee, *Curr. Appl. Phys.,* 11, **2011**, 986-988.

[33] A. Li, H. Wang, J. Han, L. Liu, *Front. Chem. Sci. Eng.,* 6:4, **2012**, 381-388.

[34] Q. Wang, H. Dong, J. H. Yu, *J. Power Sources,* 271, **2014**, 278-284.

[35] J. Wu, P. P. Sharma, B. H. Harris, X.D. Zhou, *J. Power Sources*, 258, **2014**, 189-194.

[36] I. Ali, N. Ullah, S. Omanovic, *Int. J. Electrochem. Sci*., 9, **2014**, 7198-7205

[37] F. Jia, X. Yu, L. Zhang, *J. Power Sources*, 252, **2014**, 85-89.

[38] D. Chi, H. Yang, Y. Du, T. Lv, G. Sui, H. Wang, J. Lu, *RSC Adv*., 4, **2014**, 37329-37332.

[39] R. Kas, R. Kortlever, A. Milbrat, M. T. M. Koper, G. Mul, J. Baltrusaitis, *Phys. Chem. Chem. Phys*., 16:24, **2014**, 12194-12201.

[40] D. Ren, Y. Deng, A. D. Handoko, C. S. Chen, S. Malkhandi, B. S. Yeo, *ACS Catal*., 5, **2015**, 2814-2821.

[41] C. W. Li, J. Ciston, M. W. Kanan, *Nature*, 508, **2014** , 504-507.

[42] R. Kas, R. Kortlever, H. Yilmaz, T.M. Koper, G. Mul, *ChemElectroChem*, 2:3, **2015**, 354-358.

[43] S. Lee, H. Ju, H. Jeon, R. L. Machunda, D. Kim, J. K. Lee, J. Lee, *ECS Trans*., 53:29, **2013**, 41-47.